#24-105
2024 AFS Proceedings ©American Foundry Society

Producing Castings With Nano Reinforcements—Challenges and Opportunities

David Weiss
Eck Industries (Retired), Manitowoc, Wisconsin, USA

ABSTRACT

Nano reinforcement of aluminum casting alloys can offer a significant property improvement to the base material, including high static and dynamic strengths and improved castability. There are three strengthening factors in particulate-reinforced metal matrix composites (metal matrix nanocomposites-MMNC's): 1) A load bearing effect from the particles themselves; 2) Enhanced dislocation strengthening effect; and 3) Orowan strengthening. Orowan strengthening is found to play a significant role in MMNC's, with the strengthening effect increasing with decreasing size of the nanoparticles. From a practical standpoint, the successful manufacture of MMNC's rely on three important technical achievements: 1) Getting the particles into the melt; 2) Dispersing the particles within the melt; and 3) Even dispersion of particles into the solidifying casting.

The specific objectives of this project were to develop more effective ways to deliver particles into the melt and to ensure even particle dispersion. While not all the techniques attempted were successful, significant progress was made with some of them, resulting in the production of several sample castings that demonstrated higher mechanical properties and importantly, the ability to easily cast strong, difficult to cast materials that had challenging geometries. Much of the project focused on work that would make nanocomposites affordable and producible in large batches suitable for commercial and military components.

Keywords: nanocomposites, hot tearing, alloying, ultrasonics

INTRODUCTION

Both data from the literature and previous work by the authors and collaborators suggested that the use of ultrasound might be useful for getting well dispersed nanoparticles into the melt. In small batches of ~1 kg, Li and Weiss were able to demonstrate doubling of the yield strength of common aluminum alloys by the introduction of ~2wt.% 30 nm SiC into a A356 aluminum melt using ultrasound.[1,2] However, the preparation of the melt required nearly 60 minutes/kg to do this successfully. Scaling the production of large batches of nanocomposites has been challenging. From the start of this project the focus was on large-scale manufacturing in an attempt to de-risk. A modified through-the-probe ultrasonic technique was proposed to speed up the reaction. Another approach was to use a reactive flux containing Ti and C to produce TiC nanoparticles in situ. Other techniques not included in this paper were the use of an experimental technique using an electric current to de-agglomerate particles once they entered the melt.[3] Finally, an attempt to develop a procedure to produce master alloys as a more cost effective method to add nano reinforcements into aluminum alloys was tried.

EXPERIMENTAL PROCEDURES

DEVELOPMENT OF THROUGH-THE-PROBE ULTRASONIC EQUIPMENT

A production ultrasonic degassing unit was modified to enable delivery of nanoparticles through the vibrating ultrasonic head and tested in water. This modified head unit is shown in Figure 1. The device plugged after 30 seconds due to accumulations of the ultrafine particles in the unit. The unit is designed to stop operation if the gas flow is interrupted, and continuous operation was not possible.

Figure 1. Modified ultrasonic head unit.

The “through-the-probe” addition of nanoparticles was set aside and a fluidized bed feeder was built for the addition of particles. The pressurization gas was Argon. The yellow material shown in Figure 2 is Porcerax II,® a porous steel that controlled the flow of gas and particles to a level low enough to be incorporated into the metal ultrasonically near the probe.

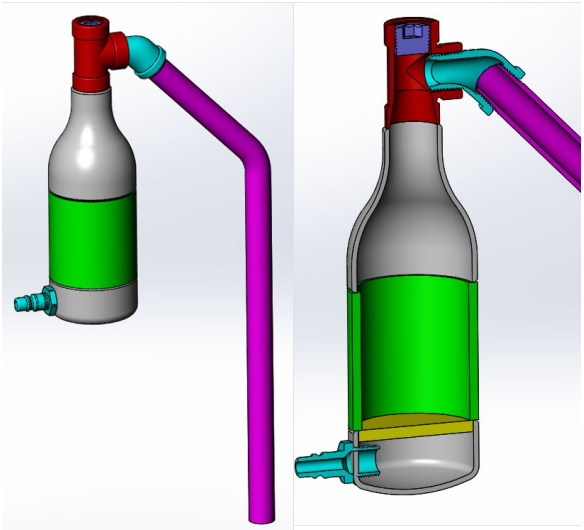

Figure 2. Fluidized bed feeder for the introduction of nanoparticles.

Water testing of this device was successful, demonstrating the ability to deliver particles uniformly (Figure 3). The fluidized bed feeder was used to successfully deliver a mixture of 50nm alumina powder into an A206 melt. The device performed as expected and is shown in Figures 3 and 4.

Figure 3. Completed particle delivery unit.

Figure 4. Fluidized particle delivery in molten metal.

The results show well distributed particles at the grain boundaries with some clustered particles in the grain. The sample was not ultrasonically processed, and the solidification rate was not very high, but the efficiency of the distribution method was demonstrated. The morphology of the copper phase was modified with the addition of the nanoparticles. It is interesting to note that the particles self-disperse in the copper phase but not in the alpha aluminum phase (Figures 5 and 6).

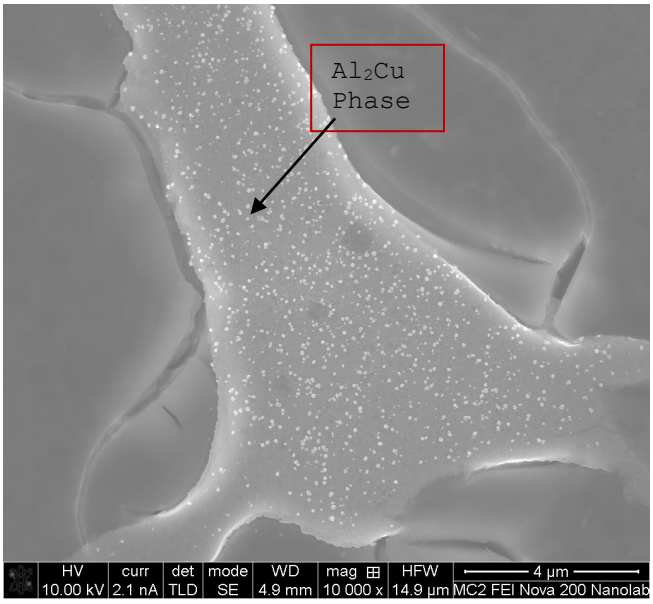

Figure 5. A206 with alumina dispersed in Al_2Cu phase.

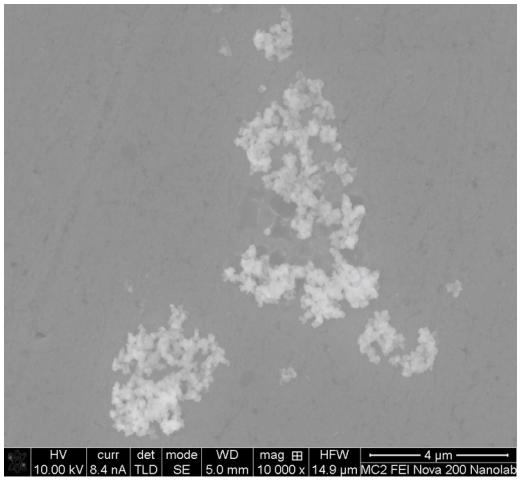

Figure 6. In-grain clustering of alumina dispersed in A206.

Some of the copper phases have a unique morphology as shown in Figure 7. This entangled phase contributes to the reduced hot tearing tendency in this alloy with the addition of nanoparticles.

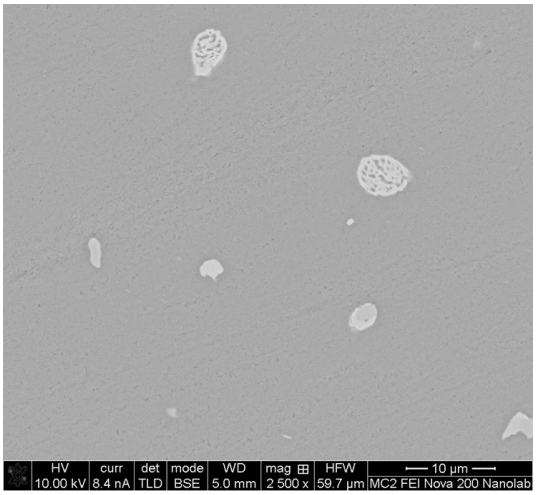

Figure 7. A round entangled Al_2Cu phase is noted in A206 containing alumina nanoparticles.

The large bubble size produced from this device resulted in many of the particles being dragged to the surface and were not incorporated. The steel delivery tube was replaced with a graphite tube with a porous plug at the end to reduce bubble size and prevent the pick-up of iron from the original tube. High-temperature seals were added to maintain pressure when the probe was used for extended periods of time in molten metal.

Three metal/particle trials were completed with the modified unit.

- A206/Alumina
- A206/TiC
- A206/BN

One of the challenges in this process was to be able to characterize the particle additions in real time. Thermal analysis was explored as an option to do this. While the interpretation of the results was inconclusive, a definite change in the tests on the 206/BN was seen. A206 was thermally tested before and after the addition of boron nitride nanoparticles. A difference was noted between the cooling rates directly following nucleation or the start of solidification. The difference in cooling rates was approximately 0.15°C/s (0.27°F/s)and is shown in the red circles of the graphs in Figure 8. This is typically attributed to a change in grain size.

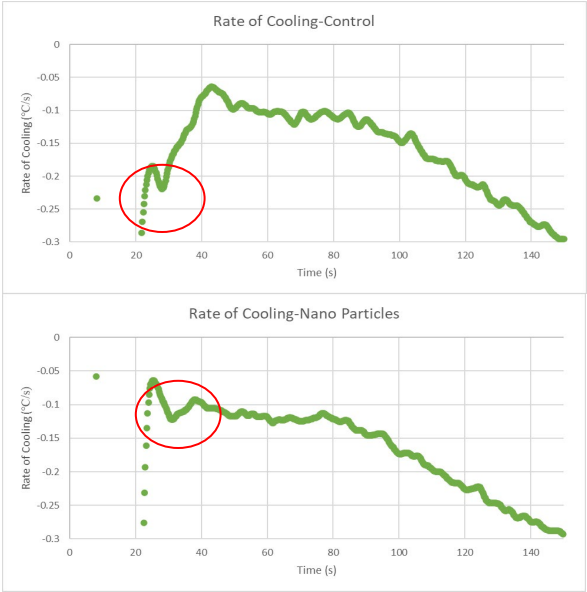

Figure 8. Difference in thermal analysis of A206 (top) and A206 with BN (bottom).

REACTIVE FLUXES

Several experiments were conducted to help determine the role of fluxes in the addition of ceramic particles into the melt. A 2% MgO 1 micron powder was added in a 33%, 67% flux mixture to 35 pounds of an Al8Ce10Mg alloy. The material was mixed with a standard impeller for one hour at 804.4C (1480F). The alloy before particle addition had average mechanical properties of 28.3 KSI tensile, 27.0 KSI yield and .8% elongation. After particle addition, average mechanical properties were 32.9 KSI tensile, 28.8 KSI yield and 1.8% elongation. This represents a 16% improvement in tensile strength, a 7% improvement in yield strength and a 225% increase in elongation.

Figure 9 shows a microstructure of the alloy before the addition of particles. Note the elongated AlCe microstructure and the magnesium pools that have formed because of the low cooling rate relative to the amount of magnesium in the alloy.

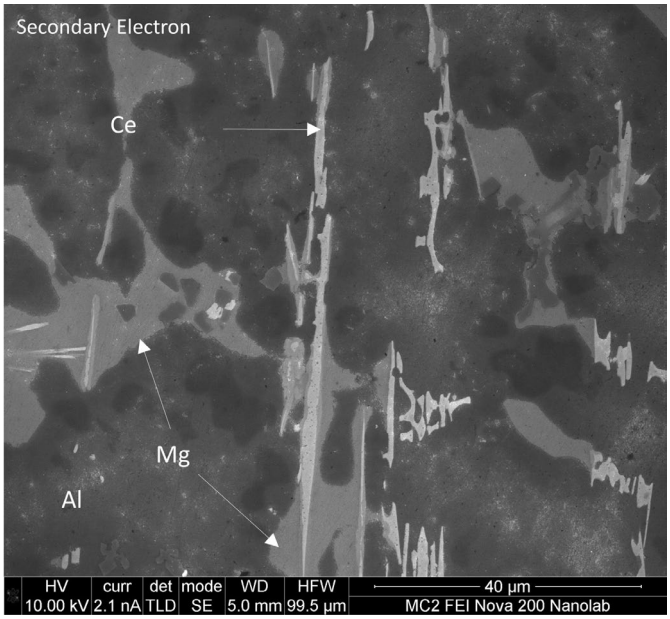

Figure 9. Al-Ce-Mg before introduction of nanoparticles.

Compare the Figure 9 structure to Figure 10. The distributed MgO as well as a major change to the aspect ratio of the AlCe intermetallic is seen. The Mg pooling is less pronounced, and the alloy looks cleaner and more homogenous. The small MgO particles act as nucleation sites for Al-Ce intermetallic as well as for the magnesium. The flux functions as it should, to remove any large oxides or inclusions from the mixing process.

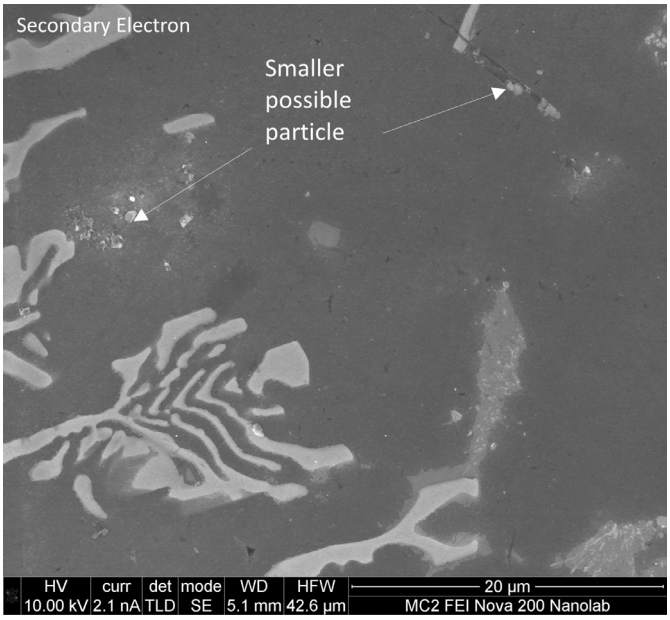

Figure 10. Al-Ce-Mg alloy after introduction of MgO nanoparticles.

A series of flux melting experiments with both reactive and non-reactive flux done in cooperation with the University of Michigan were performed at Eck Industries. The list of flux experiments completed is shown in Table 1.

Table 1. List of Flux Experiments

Raw input alloy	Processing temp. [C]	Flux/C composition	Stir processing
Al-6Ti w/SRC flux (KCl+MgCl2) + nano C (500 nm)	850	70wt% flux + 30wt% nano C	Stir w/BN coated graphite rod after 10 min
Al-6Ti w/SRC flux (KCl+MgCl2) + nano C (500 nm)	950	70wt% flux + 30wt% nano C	No stir
Al-6Ti w/SRC flux (KCl+MgCl2) + diamond C (3-10 nm)	850	70wt% flux + 30wt% diamond	Stir w/BN coated graphite rod after 10 min
Al-6Ti w/SRC flux (KCl+MgCl2) + diamond C (3-10 nm)	950	70wt% flux + 30wt% diamond	No stir
Plain P1020 w/Ti-reactive flux (K2TiF6) + nano C (500 nm)	850	95wt% flux + 5wt% nano C	Stir w/BN coated graphite rod after 10 min
Plain P1020 w/Ti-reactive flux (K2TiF6) + nano C (500 nm)	950	95wt% flux + 5wt% nano C	UA processing for ~3 min
Plain P1020 w/Ti-reactive flux (K2TiF6) + diamond C (3-10 nm)	850	95wt% flux + 5wt% diamond	Stir w/BN coated graphite rod after 10 min
Plain P1020 w/Ti-reactive flux (K2TiF6) + diamond C (3-10 nm)	950	95wt% flux + 5wt% diamond	No stir
Plain P1020 w/SRC flux (KCl+MgCl2) + 5wt% Cu + TiC (ex situ process)	850	70wt% flux + 30wt% 800 nm TiC	Stir w/BN coated graphite rod after 10 min
Plain P1020 w/SRC flux (KCl+MgCl2) + 5wt% Cu + TiC (ex situ process)	850	70wt% flux + 30wt% 40-60 nm TiC	Stir w/BN coated graphite rod after 10 min
Al-5Ti-B w/SRC flux (KCl+MgCl2) + nano C (500 nm)	850	70wt% flux + 30wt% nano C	Stir w/BN coated graphite rod after 10 min
Al-5Ti-B w/SRC flux (KCl+MgCl2) + nano C (500 nm)	950	70wt% flux + 30wt% nano C	No stir
Plain P1020 w/SRC flux (KCl+MgCl2) 5wt% Cu + TiC (ex situ process)	850	40-60 nm particles with flux on top (enough for full surface coverage)	No stir
Al-5Ti-B w/SRC flux (KCl+MgCl2) + TiC (ex situ process)	850	40-60 nm particles with flux on top (enough for full surface coverage)	No stir

A number of these flux experiments have shown promising results, particularly those done with a reactive (Ti-containing) flux. An example is shown in Figure 11 where substantial amounts of nano-sized TiC were produced. In this instance, most of the particles were pushed to the grain boundaries. This was not unexpected, given that the solidification rate was very low (0.5°C/sec [0.9°F/sec]). This is lower than typical heavy-sectioned aluminum castings. The dark spots are un-reacted carbon particles indicating that the carbon level can be reduced, or additional cleaning is required.

A key accomplishment in these trials was the establishment of processing temperatures. If the processing temperatures were too low, undesirable phases formed, such as Al3Ti that reduced mechanical properties and increased segregation of impurities. This is shown in Figure 12.

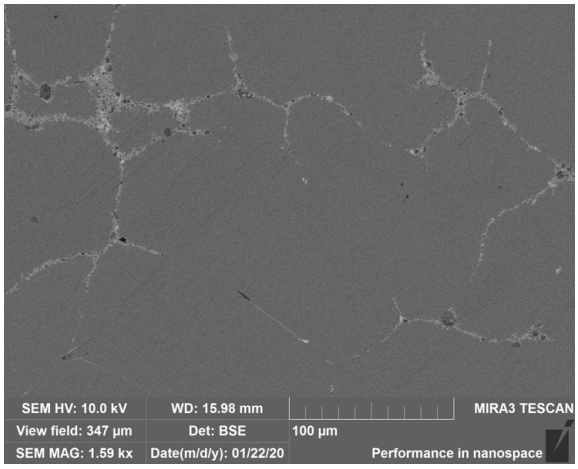

Figure 112. Results of in-situ formation of TiC reinforcement.

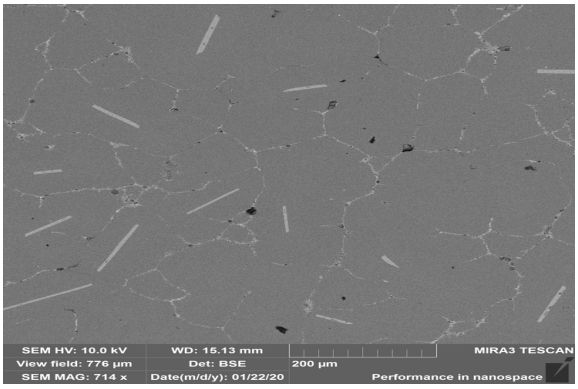

Figure 12. P1020 + K2TiF6 flux + nano C (500 nm). The elongated Al3Ti is an undesirable phase that seems to be minimized at higher processing temperatures.

Figure 13 shows the hardness values of P1020 aluminum compared with low volume fraction TiC additions. In all cases the composite shows improvement in high temperature hardness compared to the base un-alloyed material. The numbers above the figure from left to right show volume percent reinforcement, particle size and grain size. The grain size shows a significant reduction with the addition of TiC.

- D1 (0.59±0.14 vol%, 546±59 nm, 29.5±2.1 µm)
- D4 (0.60±0.21 vol%, 574±28 nm, 30.4±1.6 µm)
- D2 (0.59±0.11 vol%, 593±26 nm, 34.2±2.6 µm)
- P1020 (78.1±10.7 µm)

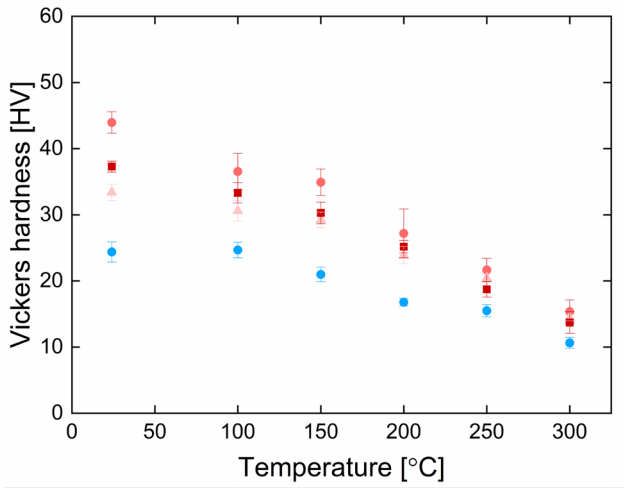

Figure 13. Hardness values of P1020 and TiC reinforced aluminum produced in-situ with flux and carbon.

MASTER ALLOY DEVELOPMENT

The development of master alloys containing nanocomposite structures is important from the standpoint of cost and ease of deployment. This project focused on the development of master alloys containing at least 7% nanoparticles via ball milling and sintering. Initially, pure aluminum powders were used along with 800 nm alumina powders and were added to A206 alloys. While this resulted in significant grain refining of the alloy, it did not improve the mechanical properties due to large amounts of undissolved master alloy in the A206 alloy. This problem is shown in Figure 14.

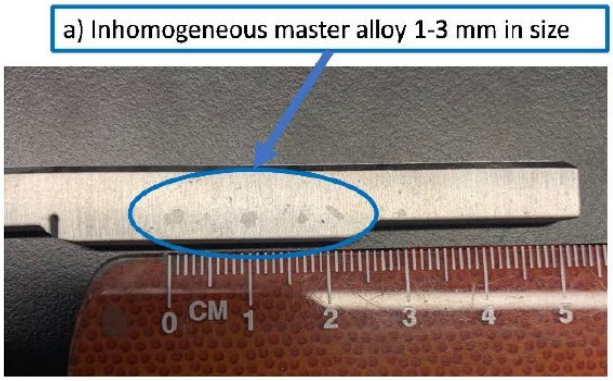

Figure 14. Undissolved master alloy in A206.

Changing the master alloy base (i.e., from pure Al powders in previous castings to Al-8Ce-10Mg powder) resulted in no visible inhomogeneous master alloy fragments. This is a significant improvement over the previous casting of A206 with 1 wt.% Al_2O_3. The comparison between the two alloys can be seen in Figure 15. The top-left cylinder is an A206 + 0.7 wt.% Al_2O_3 alloy cast earlier and the bottom-left cross-section is the Al-7Ce + 0.1 wt.% Al_2O_3 casting. The cylinder on the top-left (A206 MMC) shows that the Al-based master alloy used in the A206 alloy is visible to the human eye. The Al-based master alloy does not completely break down in the melt, resulting in inhomogeneous master alloy fragmentation. This is not the case with the Al-Ce-Mg-based master alloy.

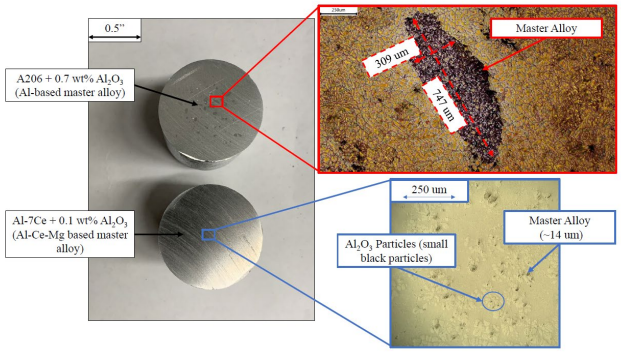

Figure 15. Optical micrographs and their respective locations comparing A206 + 0.7 wt.% Al_2O_3 and Al-7Ce + 0.1 wt. % Al_2O_3.

Optical microscopy at 100x magnification shows that a minimal amount of inhomogeneous master alloy fragments are dispersed throughout the casting. The diagonal length of these fragments was ~14 um. This is a 95-98% reduction in size compared to the Al-based master alloy used in the A206 casting. The Al-Ce-Mg powder has a much lower liquidus temperature (~600 C/1112F) compared to pure Al (~660C/1220F). This is believed to have more of an impact on the homogenous breakdown of the master alloy. Overall, it is evident that changing to an Al-Ce-Mg master alloy results in smaller and less inhomogeneous fragments of master alloy throughout the casting. It also appears to have positively affected the homogenous distribution of the nano-sized Al_2O_3 reinforcements.

SUMMARY OF WORK AND CONCLUSIONS

DEVELOPMENT OF THROUGH-THE-PROBE ULTRASONIC EQUIPMENT

Feeding nanoparticles through the ultrasonic probe is not a long-term solution since the nanoparticles plug the probe after a short period of operation. However, this led to the development of a feeding system, that when used in conjunction with ultrasonics, successfully fed and distributed the particles into the melt. In use of the developed system, the feed rate of particles is slow, about 1g per minute. A 30 kg batch size would require, assuming a desired loading of 2%, about 10 hours to prepare. This is probably objectionable except for very specialized products.

A new design was developed to deliver particles at 18 g per minute. This would reduce processing costs by an order of magnitude or more.

A206 reinforced with 2% nano-alumina

- Economics = $4-$16/lb
- Average improvement in properties = ~20%

REACTIVE FLUXES

Reactive fluxes always helped the incorporation and dispersion of particles. Low melting point fluxes when mixed with particles assist with wetting and incorporation. This speeds up the reaction. Fluxes containing Ti and carbon form in-situ TiC readily.

Process parameters need to be controlled tightly to avoid the formation of Al_3Ti or the size of the Al_3Ti needs to be reduced by processing in an electric field. More work is required to improve the economics of the process, but it shows promise. All the full-sized castings produced for this project utilized this technique.

A206 reinforced with 1% TiC

- Economics = ~$9/lb
- Average improvement in properties = ~5-20%
- With a significant reduction in hot tearing tendency

MASTER ALLOY DEVELOPMENT

Utilizing a variety of master alloy constituents and matrix alloys, it was demonstrated that master alloys of at least 7% nanoparticles can be produced and dispersed. Increasing particle loading in the master alloy will be the focus of future research. This appears to be the most cost-effective approach.

A206 reinforced with 2% nano-alumina

- Economics = ~$4-6/lb
- Average improvement in properties = ~20%

THE PATH FORWARD

While much has been accomplished in this program, there is much work ahead to optimize and commercialize these types of alloys for casting as well as to realize their potential in wrought products and in additive manufacturing. Reducing processing and ingredient costs is always a priority.

Nano-reinforced alloys should have good temperature resistance and that data needs to be quantified. Process consistency needs to be improved to deliver conforming

products consistently and the development of quality checks and metrics should be a priority for widespread military and commercial deployment.

ACKNOWLEDGEMENTS

This American Metalcasting Consortium (AMC) project was sponsored by the Defense Logistics Agency Information Operations, J68, Research & Development, Ft. Belvoir, Virginia. and the Defense Logistics Agency-Troop Support, Philadelphia, Pennsylvania.

Valuable comments and support were provided by the American Foundry Society and its Aluminum & Light Metals Division.

REFERENCES

1. Choi, H., Cho, W., Li, X.C., Hoefert, D. Weiss, D. et al., “Scale-up Ultrasonic Processing System for Batch Production of Metallic Composites,” *AFS Transactions*, Vol. 121, pp. 145-151 (2013).
2. Li, X., Yang, Y., Weiss, D., "Ultrasonic Cavitation Based Dispersion of Nanoparticles in Aluminum Melts for Solidification Processing of Bulk Aluminum Matrix Nanocomposite: Theoretical Study, Fabrication and Characterization," *AFS Transactions,* 115, pp. 249-260 (2007).
3. Goettsch, J., Gladstein, A., Weiss, D., Shahini, A., Taub, A., “Secondary Phase Refinement in Molten Aluminum via Low Power Electric Current,” *TMS Light Metals* (2023).